DESIGN AND TESTING OF AN ADAPTIVE FLAPPING WING

T. Doll[1], Th. Bein[2], T. Koch[2]
[1]Chair of System Reliability and Machine Acoustics,
Darmstadt University of Technology, D-64289 Darmstadt
[2]Fraunhofer Institute for structural Durability and System Reliability LBF,
D-64289 Darmstadt

1. MOTIVATION

"Flying like a bird" is a dream as old as mankind itself (fig. 1). But the very details of the fluid mechanical phenomena of birds flapping wings are very complex and not fully understood up to the present. Evolution tought birds to control the complex shape forms and shape variations which are necessary to enable efficient flight under variable conditions.

With this work a very first step is done into the direction of simulating and understanding these complex processes. Here an analysis by synthesis approach is performed, i.e. a system is built with similar degrees of freedom as a natural wing and the dynamic shape control during a flapping period is optimized using evolutionary algorithms.

The wing geometry has to be adaptive in order to enable online variations during windtunnel tests. In the following sections the adaptronics of the wing will be described and the effectiveness of this approach will be demonstrated.

FIG 1. Daedalus and Ikarus

Furthermore, the successful implementation of evolutionary algorithms for dynamic shape control during flight will be shown. The evolutionary algorithm is the most important part of the learning system, controlling the behavior of the actuators. Therefore no manual interaction is necessary during the adaptation process. This closed loop optimization involving variations and measurements is necessary to make the whole process feasible. At the same time, it requires a reliable adaptronic design and measurement of the fluid dynamic properties that are subject to optimization.

The adaptive wing model has to be able to twist the wing profile and the flaps have to be able to move up and down. To ensure variability, the wing was divided into four separately operable segments. Also the movement of the wing must be a waving one, comparable to a birds wing. Therefore, the trajectory over one flapping period of the following parameters was subject of the optimization:

– the frequency of the wave
– the twisting angles of the four segments
– the angular positions of the flaps of the four segments

In total, the time courses of nine parameters have to be optimized during one cycle.

2. FIRST DESIGN ATTEMPT

The first intent to accomplish the twist of the wing was to use the tension-torsion coupling of the wing's skin. The wings skin consists of GRP, and if the direction of the angle of the fiber is chosen in the right way it is possible to twist the wing by a strain in the longitudinal direction. The twisting angle is also dependent on the stiffness of the fiber composite and the force that will be needed to deform the wing. To gather basic information about the dependencies an FE model of the skin was developed. The direction of the fiber, the thickness of the composite, and the amount of strain served as input. The results of the simulation were the twisting angle and the force that is needed to deform the wing.

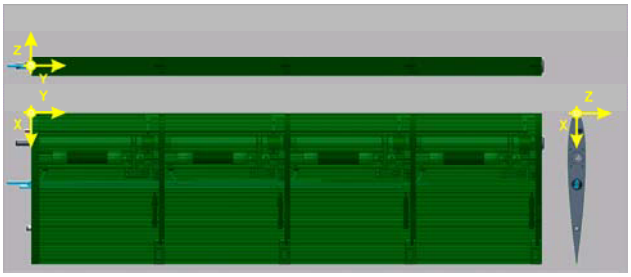

FIG 2. Coordinate system of the wing geometry

The profile of the wing is a so-called 4-digit NACA 0012 profile (fig. 2). The first digit represents the relative camber. The second digit represents the camber position. The third and fourth digits represent the thickness (see e.g., Truckenbrodt, Schlichting [1]). The NACA 0012 is a symmetric profile and the thickness of 12% is chosen because of its stable behavior even at large incidence angles. The results of the simulations show that it is theoretically possible to twist the wing by tension-torsion coupling by a maximum angle of about 2 degrees.

But the forces required to deform the wing are much too

large for piezoceramic actuators, which create large forces, but only a small strain. The fiber composite must be very stiff to produce the required twisting angle, even taking into consideration that the force required to deform the wing gets much too large. Therefore bigger actuators would be needed, but this is against the demand of low costs of the actuator system. The idea of using hydraulic systems was ruled out, because of the weight and the absence of hydraulic supply systems at the wind tunnel.

3. NEW DESIGN AND INITIAL OPERATION

3.1. Fluidic Muscle Actuator

To solve the above mentioned problem an actuator had to be found that produces much more strain and at the same time provides enough power to twist the wing. One possible actuator is a so called Fluidic Muscle™ by FESTO. It works with pressurized air and is able to generate a force of about 1500 N. The strain that can be generated with this force is about 1% of its length. Unfortunately, it can generate only tensile loads. Therefore a mechanical gear is required to transform the tensile force into a torsional moment without too much loss in performance. This can be accomplished with flexure hinges, which are described later on. First it was checked if the generated force is able to twist the wing. This is done by FEM calculations. In the simulation the force is split into two equal parts. One part of the force is applied at the top of the thickest part of the profile. The direction of this force is in negative x-direction (compare fig. 2). The second part is applied at the bottom of the thickest part of the profile. The direction of this force is in positive x-direction. The simulation result for one segment can be seen in fig. 3. The results indicate that it is possible to twist the wing with a fluidic muscle. Proportional pressure regulators (VPPE by FESTO) are used to drive the muscles.

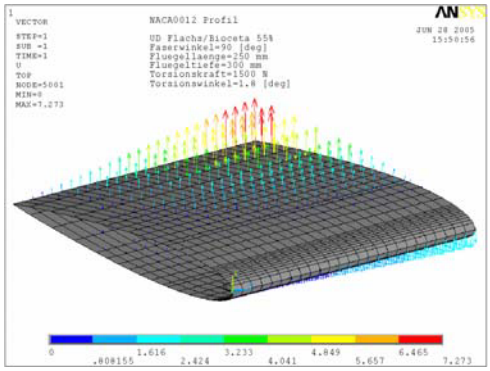

FIG 3. Displacement of the wing profile when a torsion force of 1500 N is applied

It turned out that the performance of the proportional pressure regulators was too slow to exhaust the air. This lessened the predicted dynamic behavior of the wing and the flapping frequency had to be reduced to 0.5 Hz.

3.2. Flexure Hinges

As mentioned before the tensile force must be transformed into a torsional moment. One possible solution could have been a screwthread. It was, however, assumend that the performance loss of the Fluidic Muscle™ would be too high due to friction losses.

Another possible way is the use of flexure hinges which work without friction and without play. So the movement is led directly to the wing without losses. It is also possible to convert a linear movement into torsion.

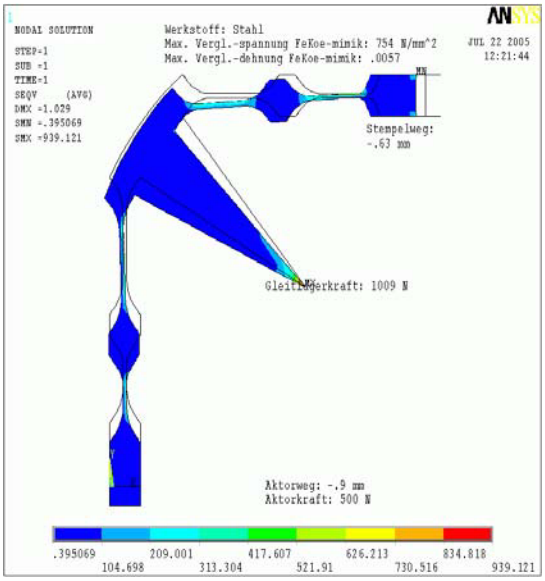

FIG 4. Displacement and stress of the first flexure hinge

To design flexure hinges and to make the correct assumptions some experience of flexure hinges and several FEM simulations are needed. Several geometric parameters influence the movement of the flexure hinge, which depends on the movement of the driving section and of the driven section of the hinge. Finally the performance of the construction depends on the achieved magnification factor.

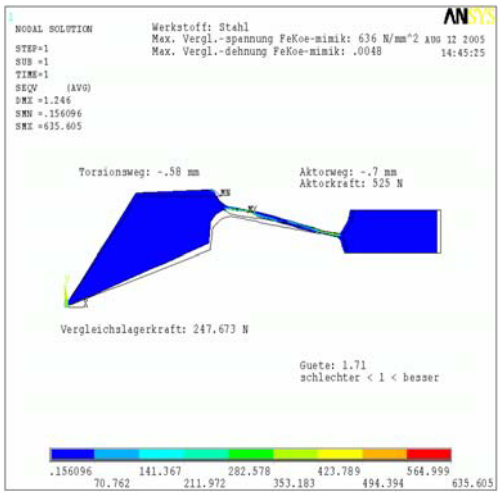

FIG 5. Displacement and stress of the second flexure hinge

First the linear movement of the fluidic muscle is transferred from the x-axis to the y-axis with one flexure hinge arrangement. The displacement and the stress can be seen in fig. 4. Another hinge attached to the first one transfers the linear movement from the y-axis into a rotation around the x-axis. The displacement and stress can be seen in fig. 5. Results show that the stress is

tolerable in both cases if the right material is chosen. The used material is spring steel 50CrV4. The design of the complete flexure hinge arrangement can be seen in fig. 6.

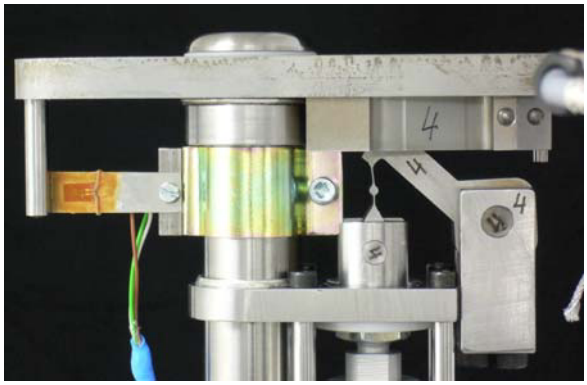

FIG 6. Complete flexure hinge arrangement

At the bottom of fig. 6 the top of the Fluidic Muscle™ can be seen, which pulls down the first flexure hinge arrangement as it contracts. This hinge is pivoted on the right side and so the upper right corner of the first hinge arrangement turns left. To guarantee a linear motion of the two ends of the hinge arrangement without exceeding the stress limits, the top-down-hinge and the left-right-hinge both consist of two hinges. With that construction the bending stress could be relieved better.

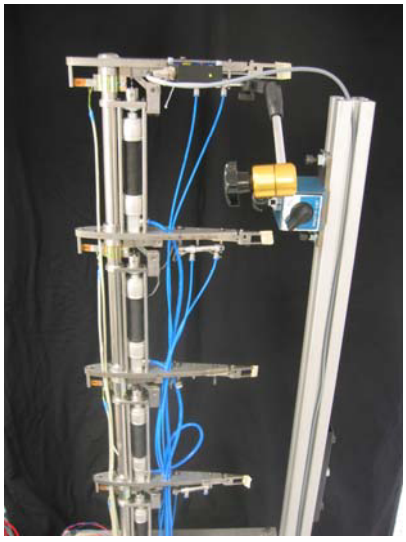

FIG 7. Complete wing interior at test rig

The second hinge arrangement also consists of two hinges with a small lever between them. The right section is moved to the left by the first hinge arrangement. The upper left side of the hinge is fixed at the fin with two pins and the fin is pivoted at the spar (compare to fig. 9). The fin is turned around the bar and the skin of the wing is twisted. Every module is fixed to the previous fin and the first module twists the whole segments two to four. The second module twists the whole segments three to four and the third module twists the whole segment four (compare fig. 7).

3.3. Flap Movement

For the positioning of the rear flaps, pneumatic round cylinders (type DSEU by FESTO) are used. Leverages and bowden wires are used in order to convert the longitudinal movement of the cylinders into an angular motion of the flap. The positioning of the actuators is controlled by proportional directional control valves (MPYE by FESTO).

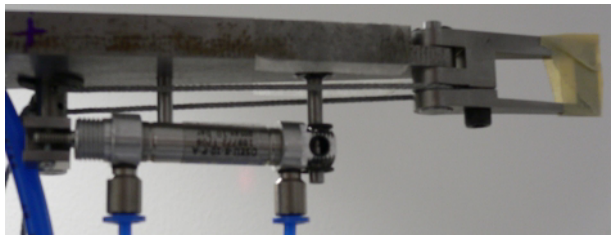

FIG 8. Design of the rear flap mechanism

3.4. Sensors and Measurement

The positions of the rear flap and the twisting of the profile of the four segments are measured by resistance strain gages bonded to bending bars (see fig. 6). Since only small twisting and rotational angles have to be considered (max. 2° twisting per segment of the profile and about ±3° maximum rotation of the leverage for the positioning of the rear flap) the measured strain at the surface of the bending bars can be considered as nearly proportional to the angular position. The signals of the strain gages are amplified with a MAS MICRO II™ of SWIFT GmbH to prepare the signals for use in the closed loop control system.

4. SETUP AND WIND TUNNEL EXPERIMENTS

4.1. Experimental Setup

During the flapping of the wing the target positions of the actuators are permanently altered in order to achieve optimal performance. The positions are determined by optimization algorithms on the basis of evolutionary strategies which are included into a Simulink model. Inside the wind tunnel the wing is fixed onto a mounting which emerges from an opening in the bottom of the measuring section (fig. 9). The mounting itself is attached to a six component balance situated underneath the wind tunnel. Thus the wing is decoupled from the measuring section and stands free on the balance. The data collected by the balance is computed and the aerodynamic forces (ascending, resisting, lateral force) and moments (pitching, yawing and rolling moment) are derived. Depending on the optimization problem, the relevance of the loads can vary. E.g. for minimizing the ascending force of the wing, the fitness of the individuals of the evolutionary algorithm only depends on the measured data of the ascending force.

In order to generate the analog signals for control of the proportional valves and regulators and for streaming purposes of the sensor signals, a digital signal processing system (DSP-system) by dSPACE is used. With dSPACE and the associated interface software ControlDesk, the experiment can be coordinated completely from the PC. For adjusting the set point values, a simple displacement feedback controller is programmed in Simulink and downloaded onto the processor module of the dSPACE system. All internal conditions of the controller can thus be

observed and changed within the ControlDesk GUI (fig. 13).

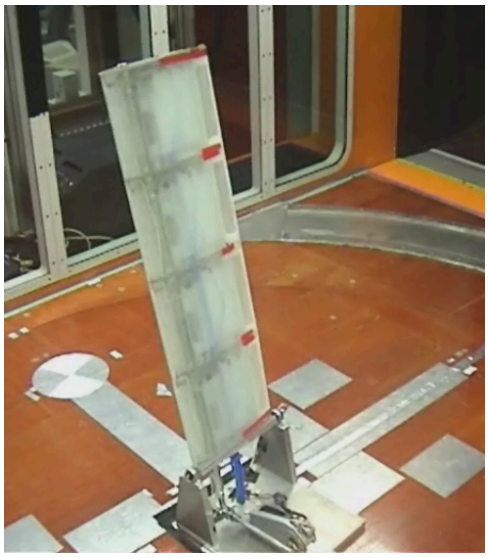

FIG 9. Adaptive Flapping Wing in Wind Tunnel

The angular position adjustment of the twisting of the wing and the rear flaps is realized by a digital PID controller, which is included in the dSPACE environment.

4.2. Simulink-dSPACE Interaction

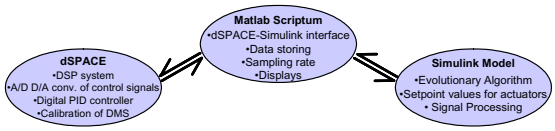

FIG 10. Simulink-dSPACE interaction

As previously mentioned the optimized positions for twisting the profile and angular positioning of the rear flaps are calculated by use of evolutionary control strategies which are implemented in a Simulink model. The set point values are then transmitted to dSPACE and the actuator positions are adjusted by the PID controller, which runs on the processor board of the dSPACE system. The data exchange between the Simulink model which contains the evolutionary algorithm and the dSPACE controller is coordinated via a Matlab program. The angular setpoint values which are calculated by the Simulink model are sent to the dSPACE system. Vice versa sensor data is collected for visualization purposes. In the following, the Simulink-Matlab-dSPACE interaction and the various functions of the modules will be briefly explained.

As illustrated in fig. 10 the Matlab program has to fulfill several tasks. Firstly it coordinates the data exchange between the Simulink model, where the set point values are calculated, and the dSPACE system, where the analog control signals for driving the actuators are generated. Within the sample time step the actual sensor data provided by the strain gages is collected and passed to the Simulink model. With this information new twisting and rotational angles are calculated and sent back to the dSPACE system. Secondly the sampling time is defined by means of Matlab timer object [2], thus controlling the data exchange from within the interface program. A graphical user interface (GUI) facilitates the use of the program. So the experiment can easily be started and suspended and some experimental data can be observed in real time (fig. 11).

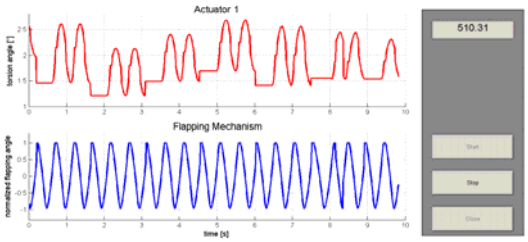

FIG 11. Matlab GUI for experiment control; above: torsion of the first segment of the wing profile; below: angular position of the flapping mechanism

The calculation of the set point values takes place inside the Simulink model. The new positions are derived via evolutionary optimization strategies. The acquired data is delivered by the six component balance, whereto the wing is attached. The aim is the minimization of a cost function which is previously defined as an optimization goal (e.g. minimum ascendancy). With the dSPACE DSP system the predetermined actuator positions are adjusted and sensor data is processed.

For the minimization of the control deviation and rapid adjustment of the set point values the parameters of the digital PID controller were tuned beforehand. Furthermore the strain gages were calibrated before the experiment. These tasks are handled by the GUI which is programmed with the associated ControlDesk software.

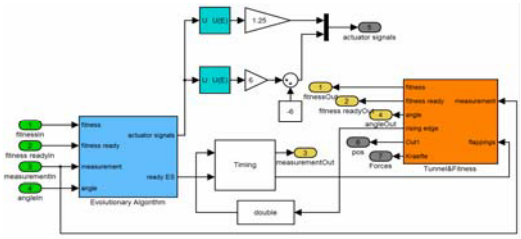

FIG 12. Simulink model: set point value calculation applying evolutionary strategies

The sampling rate of the data transfer between the Simulink model and dSPACE was set to 100 Hz. The model is permanently held in compiled state after the experiment is started and is “pushed further” with every time step by the Matlab interface program. Applying this method the Simulink model is executed in real time, which is inevitable due to the experiment control purpose. The drawback of this procedure is that all inner states of the optimization method have to be stored, because the feedback loop has to be closed by the Matlab program. Due to the problem that the local variables of the model are cleared after every time step, feedback paths lead to inconsistencies and control has no effect. Therefore the feedback parameters have to be read out at one time step and handed back at the next time step (see fig. 12 Simulink model: yellow outputs and green inputs: fitness, fitness ready, measurement, and angle).

4.3. Digital PID

In fig. 13 the model containing the data connections to the optimization routine and the digital controller for actuator positioning is shown. This model is programmed with Simulink and must be downloaded to the processor module of the dSPACE DSP-system.

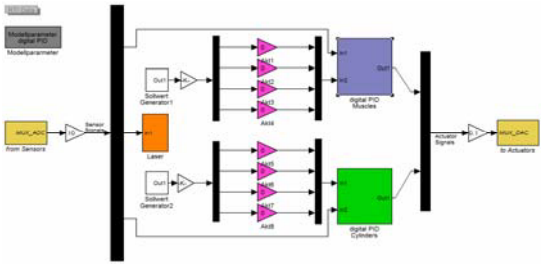

FIG 13. Simulink block diagram containing digital PID controllers for download to the dSPACE processor module

The yellow colored blocks symbolize the digital to analog conversion of the actuator signals (to actuators) and the analog to digital transformation of the sensor signals (from sensors). The set point values from the optimization routine are passed to the magenta colored gain blocks, whereby the labels Akt1 to Akt4 represent the four Fluidic Muscles™ of the four wing segments and Akt5 to Akt8 stand for the pneumatic cylinders. The blocks labeled “digital PID” contain the PID controllers for the fluidic muscles (blue) and for the cylinders (green). The orange “Laser” block is included for calibration purposes of the strain gage sensors using a laser proximity sensor. Fig. 14 shows the GUI for accessing the control and calibration parameter.

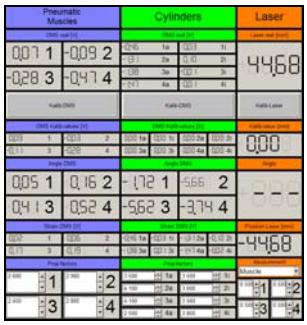

FIG 14. ControlDesk GUI (dSPACE interface)

4.4. Optimization results

Experiments are performed with variations of the quality function and the optimization method used. The experimental results which are presented here are results of an optimization run minimizing the forces on the wing. For that reason the lift and drag forces of the wing are measured during the whole flapping period of the wing with a frequency of 100 measurements per second and summed up. In order to reduce the measurement noise the summation was done during two periods of movement. The wing profile is placed in such a way that the inflow angle of the flow is $\alpha = 6$ degree. The flow velocity is set to $v = 16$ m/s. In order to estimate the noise generated by the measurement facility and the instationarities of the flow the quality variations were measured without any modification of the wing at first. The results are shown in fig. 15 indicated by the dark line. This noise level will determine the expected distance of the best solution to the absolute minimum of the quality value. The green curve shows the measured fitness during the optimization run. With a flapping frequency of $\lambda_{wing} = 0.5$Hz the measurement time for the whole optimization was about 30 minutes. It can be seen, that the quality value which is calculated by the forces on the wing is reduced during the optimization to about one third of the initial value. During the first 50 evaluations, which is equivalent to the first 10 generations of the evolution strategy the quality value is not decreased. This is explained by the strategy parameter, which is adapted during this phase to sensible values. After that the quality measure is minimized by the optimization algorithm during the next 100 evaluations. Now, the measured forces are in a range of the measurement noise and no further progress can be possible.

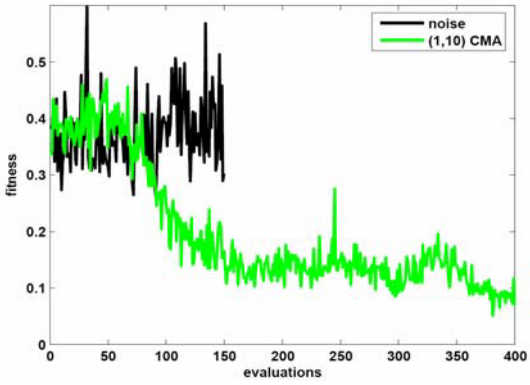

FIG 15. Measured quality of the initial design during 150 evaluations (dark) and the history of the fitness values during the optimization for 400 evaluations.

5. OUTLOOK

In view of a fully *morphing* wing, the main challenges are suitable, miniaturized but high power actuators and the highly deformable skin. For the latter, the main challenge is the high strains in the material easily exceeding the allowable strains of standard materials such as metals or CFRPs. Also buckling of the skin needs to be avoided at any circumstances. The most obvious concept is the use of an elastomer as skin material. This material can easily be deformed with low forces and can endure high mechanical strains. But since the material is rather soft, a continuous and smooth deformed surface cannot be controlled. The buckling-like deformation of the skin will even be enhanced by soft materials. Another concept is the use of glass fiber reinforced plastics (GFRP) in very thin layers which are stacked together to realize a sufficient high bending stiffness. In order to allow high strains, the individual layers must be very thin (in the order of 100 μm) and not be connected with each other. In doing so, the thickness is reduced leading to reduced strains in each layer. Those layers must be fixed and pre-strained at the boundary, on the one hand to mount them in the support, on the other hand to withstand the aerodynamic forces working on the outer layer. Otherwise, the aerodynamic forces would deform the outer layer uncontrolled. More promising is the use of smart materials in the skin itself. Shape memory alloys in their superelastic

state e.g. allow reversible strains of up to 8%. Theoretically, the skin could be manufactured from superelastic SMA as a whole. But the technology to provide thin sheets of SMA in the required size is not available, yet. To overcome technological restraints, thin wires of SMA can be used of which a mesh is build-up. With a suitable resin, an SMA composite can be realized having on the one hand a defined stiffness and on the other hand having the superelastic properties of SMA. With respect to ageing, no data is available whether such a composite undergoes ageing or creeping when cycled. Finally, shape memory polymers (SMP) can be used as skin material. These materials can be deformed arbitrarily when heated. Strains in the order of 100% can be introduced without damaging the material. When cooled down, the material keeps its deformed shape which makes it very interesting for quasi-static shape changes as required in aerodynamic applications. To bring it back into a new shape, the material must be heated and deformed accordingly. In the SMP heat wires and sensors for a controlled heating can be embedded. Again, no data on ageing and creep are available. Nevertheless, both latter concepts seem to be most feasible for a highly deformable skin.

In view of the required actuators, it is reasonable to assume that a fundamental technical amplification mechanism and/or force redirection mechanism has to be applied. While considering such mechanisms also the commercially applied amplification mechanisms or principles should be taken into account. Highest potential for built-in actuator systems are showing ultrasonic and inchworm motors due to their capability of large displacements at moderate forces with a small built-in volume and high accuracy at the same time. Other concepts would fulfill the requirements with respect to stroke, force and partly to built-in volume but have disadvantages in the other criteria. Another advantage compared to the other known actuator concepts is that they are controlled electrically rather than by heat or by fluids.

6. SUMMARY

The article shows the design of an adaptive flapping wing, including the control, the implementation at a wind tunnel and the optimization of the shape of the wing profile.

The motivation was an optimization tool by Honda Research Institute that is able to handle several parameters during a duty cycle. The demonstrator has to be descriptive, not too complex, and not too expensive. So the idea was to build up a demonstrator that has the capability to imitate the bird flight. The wing of a bird is flapping, it can be twisted continuously and it has trailing edge flaps. The presented wing approximates all of these capabilities by four segments.

During the design process the first choice to activate the twisting was a piezo actuator driven tension-torsion coupling. This was a disappointment, because of the small strain of piezo actuators. By means of the small strain, too large forces should have been generated and the piezo actuators would have become too big and expensive.

So Fluidic Muscles™ are used. They provide less force but much higher strain. The produced force is not large enough to twist the wing by the tension-torsion coupling, but it is large enough to twist the wing by a gear of flexure hinges.

The flexure hinges are designed to transform the longitudinal movement of the Fluidic Muscles™ into a rotational movement of the wing. Both, the Fluidic Muscles™ and the flexure hinge arrangements are small enough to fit into the small installation space of a NACA 0012 profile. The movement of the trailing edge flaps is accomplished with small pneumatic round cylinders. Leverages and Bowden wires convert their longitudinal movement into an angular movement of the flaps.

The position of the twisting and the trailing edge flaps is detected by strain gages bonded to bending bars. A computer system consists of Matlab, Simulink and dSPACE is used to read out the data of the sensors, processing the data, optimizing the shape of the profile and to control the actuators. The optimization is done by an evolution algorithm that is also implemented in a Simulink model. The basic principles and strategies of this algorithm and the use to the flapping wing are shown. One optimization experiment was presented, where a reduction benefit to one third of the initial value was achieved.

Although the dynamics of the flapping wing and the range of variation of the twisting angle were limited, the air stream properties of the adaptive wing were improved significantly by use of a proper optimization strategy. If the dynamics and the range of variation of the wing are further improved, it is also possible to improve the air stream properties. For a redesign the potential to improve the behavior of the adaptive wing is identified. One subject is the replacement of the valves of the Fluidic Muscles™. They exhaust the air to slow and so the flapping frequency is limited to 0.5 Hz. If faster valves are used, higher dynamics can be achieved. The reduction of the weight is an additional possibility of improvement. The fins are manufactured out of steel that could be replaced by GRP. This would improve the dynamics of the flapping mechanism, too. To improve the range of variation of the wing other actuators and/or gear mechanisms should be examined.

7. ACKNOWLEDGEMENTS

The adaptive flapping wing was developed in collaboration with the researchers of the Honda Research Institute Europe GmbH in Offenbach, who developed the evolutionary optimization routines which were applied during the project. The wind tunnel tests took place in Darmstadt- Griesheim at the facilities of the chair of Fluid Mechanics and Aerodynamics of Darmstadt University of Technology.

8. LITERATURE

[1] H. Schlichting, E. Truckenbrodt. Aerodynamik des Flugzeuges, Springer-Verlag 1967
[2] N.N. Matlab User Guide, The MathWorks Company
[3] D.B. Fogel. Evolutionary Computation. IEEE Press, 1995.
[4] H.-P. Schwefel. Evolution and Optimum Seeking. John Wiley & sons, New York, 1995.